

# Calculating the Lattice Dynamics in the $R\text{Fe}_3(\text{BO}_3)_4$ Crystals in the Quasi-Harmonic Approximation

M. S. Pavlovskii<sup>a, b, \*</sup> and N. D. Andryushin<sup>a, b</sup>

<sup>a</sup> Kirensky Institute of Physics, Krasnoyarsk Scientific Center, Siberian Branch, Russian Academy of Sciences, Krasnoyarsk, 660036 Russia

<sup>b</sup> Siberian Federal University, Krasnoyarsk, 660041 Russia

\*e-mail: mspav@iph.krasn.ru

Received May 22, 2019; revised May 22, 2019; accepted June 10, 2019

**Abstract**—The frequencies of lattice vibrations in the  $R\text{Fe}_3(\text{BO}_3)_4$  ( $R = \text{Pr, Nd, Tb, Dy, or Ho}$ ) crystals in the high-temperature  $R32$  phase and their temperature dependence have been calculated using the quasi-harmonic approximation. It has been found that, at the boundary point  $\Lambda$  of the Brillouin zone, the frequency of the unstable vibration mode the structural phase transition  $R32 \rightarrow P3_121$  is related to strong changes with temperature in the  $\text{TbFe}_3(\text{BO}_3)_4$ ,  $\text{DyFe}_3(\text{BO}_3)_4$ , and  $\text{HoFe}_3(\text{BO}_3)_4$  crystals. With increasing temperature, the frequency of the soft mode stabilizes and takes a real value. No significant changes in the phonon spectra, including the boundary point  $\Lambda$ , with increasing temperature for the  $\text{PrFe}_3(\text{BO}_3)_4$  and  $\text{NdFe}_3(\text{BO}_3)_4$  crystals have been observed.

**Keywords:** lattice dynamics, structural instability, ab initio calculations, phase transitions

**DOI:** 10.1134/S106378341911026X

## 1. INTRODUCTION

The crystal structure of the  $R\text{Fe}_3(\text{BO}_3)_4$  compounds ( $R$  is the rare-earth ion) with symmetry sp. gr.  $R32$  and one molecule in the unit cell belongs to the structural type of the natural mineral huntite [1]. Upon temperature variation, the  $R\text{Fe}_3(\text{BO}_3)_4$  crystals with  $R = \text{Eu–Er, Y}$  undergo an extraordinary structural phase transition of the type of displacement from the phase with symmetry sp. gr.  $R32$  to the phase with sp. gr.  $P3_121$  [2, 3]. The extraordinary character of this phase transition is that, during it, the point symmetry (sp. gr.  $D3$ ) of the crystal does not change and only the translational symmetry changes and the cell volume increases by a factor of 3. Depending on the rare earth ion, the transition temperature changes in a very wide (from 88 to 450 K) range [2]. In the crystals with  $R = \text{La–Sm}$ , the structural transition was not experimentally observed. It is important that, at the phase transition, the point symmetry of the local environment of the rare-earth ion changes: the point group  $D3$  is in the  $R32$  phase and the point group  $C2$  is in the  $P3_121$  phase. This fact can apparently be reflected on the difference of the magnetic, magnetoelastic, and magnetoelectric properties of the compounds with groups  $R32$  and  $P3_121$  at low temperatures.

The anomaly in the temperature behavior of specific heat in the  $R\text{Fe}_3(\text{BO}_3)_4$  crystals corresponding to the structural phase transition was observed in [2]. In

[3], the  $\text{GdFe}_3(\text{BO}_3)_4$  crystal lattice dynamics was studied by Raman spectroscopy. Below the temperature of the structural phase transition, the soft mode was restored from the low-frequency region to frequencies of  $50\text{--}60\text{ cm}^{-1}$  ( $6\text{--}8\text{ meV}$ ). The similar Raman spectroscopy data were obtained for other crystals in this family experiencing the phase transition  $R32 \rightarrow P3_121$  [4]. In [5], the changes in the IR spectra during the phase transition were recorded.

Previously [6], we calculated the phonon spectrum of a  $\text{HoFe}_3(\text{BO}_3)_4$  crystal in the high-temperature phase with symmetry sp. gr.  $R32$  (the calculation was made using the nonempirical model of polarizable ions). In the vicinity of the boundary point  $\Lambda$  ( $\mathbf{q}_\Lambda = 1/3(\mathbf{b}_1 - 2\mathbf{b}_2 + \mathbf{b}_3)$ , where  $\mathbf{b}_1$ ,  $\mathbf{b}_2$ , and  $\mathbf{b}_3$  are the vectors of the reciprocal lattice) of the Brillouin zone, the anomalous softening of one of the transverse acoustic modes was found. It was shown that the distortion in the  $R32$  phase of holmium ferroborate relative to the eigenvector of such a mode yields sp. gr.  $P3_121$  with three molecules in the unit cell, which corresponds to the experimentally observed structure below the temperature of the transition in this crystal.

In [7], the crystal lattice dynamics in the  $\text{TbFe}_3(\text{BO}_3)_4$  crystal was studied using inelastic neutron scattering in the temperature range of  $180\text{ K} < T < 350\text{ K}$ , including a structural transition temperature of 192 K. A significant yet incomplete softening of the

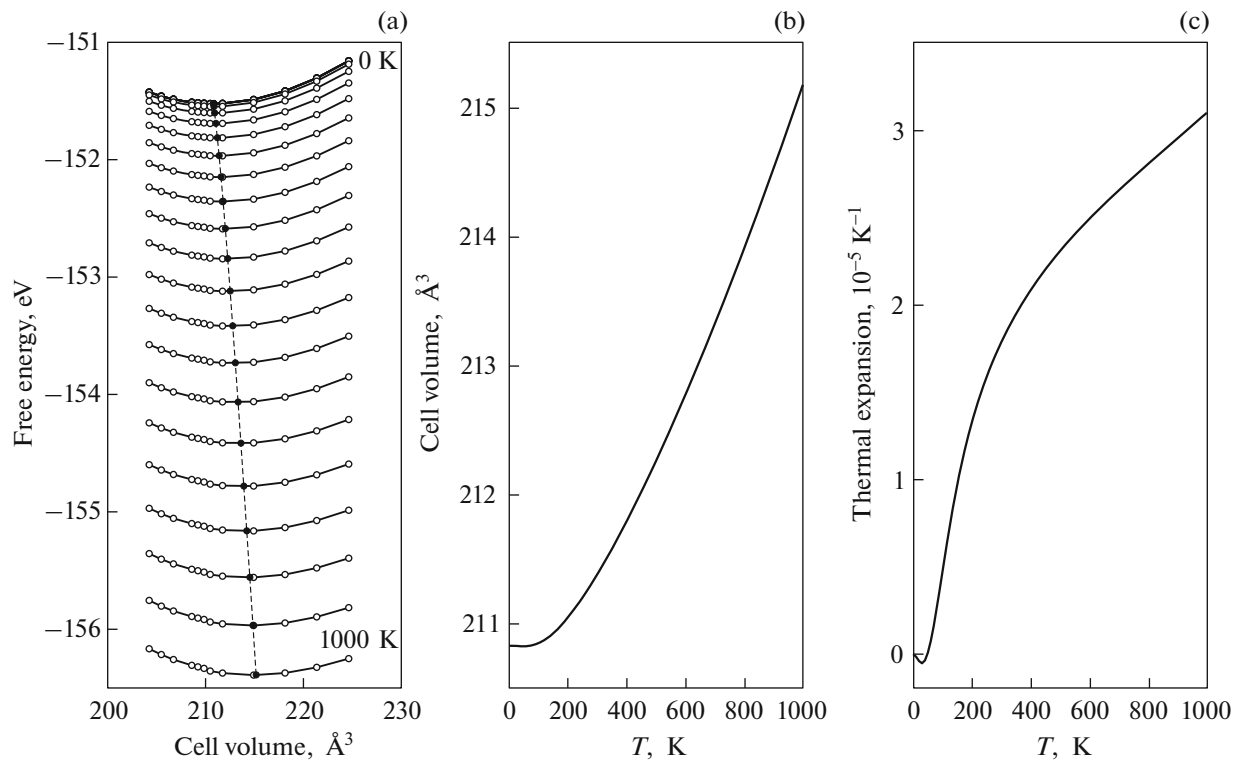


**Fig. 1.** (a) Dependence of free energy on the volume at temperatures from 0 to 1000 K. Closed circles show the minimum volumes for each curve. (b) Temperature dependence of the unit cell volume. (c) Temperature dependence of the thermal expansion coefficient.

transverse acoustic branch of the vibrations in the vicinity of the zone point  $\Lambda$  was experimentally obtained.

In [8], the crystal lattice dynamics of the  $R\text{Fe}_3(\text{BO}_3)_4$  ( $R = \text{Pr}, \text{Nd}, \text{Sm}, \text{Gd}, \text{Tb}, \text{Dy}, \text{or Ho}$ ) compounds in the high-symmetry phase (symmetry sp. gr.  $R32$ ) was calculated. The significant changes in the spectra of the compounds with different rare-earth ions were obtained only in the vicinity of the boundary point  $\Lambda$  of the Brillouin zone for acoustic branches of the vibrations. The acoustic mode frequency softening at the point  $\Lambda$  was found in all the compounds under study, including those without structural phase transition. It was found that this frequency depends on the rare-earth ion type and decreases from the compound with Pr to the compound with Ho down to imaginary values.

In this study, we estimate the temperature effect on the phonon spectra of the  $R\text{Fe}_3(\text{BO}_3)_4$  ( $R = \text{Pr}, \text{Nd}, \text{Tb}, \text{Dy}, \text{or Ho}$ ) crystals by calculating the lattice dynamics in the harmonic approximation, but using the lattice parameters and atomic coordinates corresponding to a specified temperature. To do that, the temperature dependence of the unit cell volume and thermal expansion coefficient were calculated in the quasi-harmonic approximation [9].

## 2. CALCULATION TECHNIQUE

The calculation was made using the density functional theory with the Perdew–Burke–Ernzerhof exchange–correlation functionals with the generalized

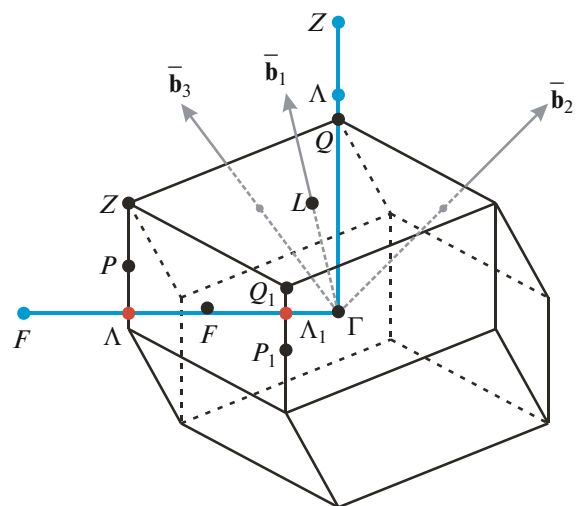


**Fig. 2.** Brillouin zone for the rhombohedral lattice. Gray arrows show the directions along which the dispersion curves were calculated.

gradient approximation (PBE–GGA) implemented in the VASP package [10, 11]. The number of plane waves was limited by an energy of 600 eV. The  $7 \times 7 \times 7$  Monkhorst–Pack mesh [12] was used. In the calculation, we used the GGA +  $U$  method in the Dudarev approximation [13] for iron with  $U = 4$  eV. To calculate the vibration frequencies, a  $2 \times 2 \times 2$  supercell was built and force constants were calculated by the method of small displacements implemented in PHONOPY [14]. The Helmholtz free energy calculation in the quasi-harmonic approximation was also made using the PHONOPY software [9].

### 3. RESULTS AND DISCUSSION

We calculated the equilibrium lattice parameters and atomic coordinates of the  $\text{PrFe}_3(\text{BO}_3)_4$  crystal in the  $R32$  phase with disregard of temperature. The Helmholtz free energy and its temperature dependence were calculated for twelve different unit cell volumes using formula (1) (we used the cell volume larger and smaller than the equilibrium value; for each fixed volume, the lattice parameters and atomic coordinates corresponding to the minimum internal energy were calculated), where  $E_{\text{static}}$  is the total internal energy of the crystal;  $\mathbf{q}$  and  $\nu$  are the wave vector and branch number, respectively;  $\omega_{\mathbf{q},\nu}$  is the oscillation frequency; and  $T$  is the temperature. The dependences of the free energy on the volume corresponding to specific temperatures were plotted (the curves were calculated with a step of 10 K); some of them are shown in Fig. 1a. At each temperature, the cell volume corresponding to the minimum free energy was determined, which made it possible to plot the temperature dependence of the unit cell volume (Fig. 1b) and calculate the thermal expansion coefficient (Fig. 1c)

$$F = E_{\text{static}} + \frac{1}{2} \sum_{\mathbf{q},\nu} \hbar \omega_{\mathbf{q},\nu} + k_{\text{B}} T \sum_{\mathbf{q},\nu} \ln \left( 1 - \exp \left( \frac{-\hbar \omega_{\mathbf{q},\nu}}{k_{\text{B}} T} \right) \right). \quad (1)$$

Taking into account the proximity of the structural and chemical properties of rare-earth ferrobates and the impossibility of using imaginary values of the crystal lattice vibration frequency in calculating the free energy (in the  $\text{PrFe}_3(\text{BO}_3)_4$  crystal, there are no imaginary modes) for the  $\text{NdFe}_3(\text{BO}_3)_4$ ,  $\text{TbFe}_3(\text{BO}_3)_4$ ,  $\text{DyFe}_3(\text{BO}_3)_4$ , and  $\text{HoFe}_3(\text{BO}_3)_4$  crystals, in further calculations the thermal expansion coefficient was taken equal to the thermal expansion coefficient calculated for  $\text{PrFe}_3(\text{BO}_3)_4$ . This allowed us to calculate the temperature dependence of the unit cell volume for all the investigated compounds.

For each of the investigated crystals in the  $R32$  phase, the lattice dynamics was calculated using the lattice parameters and atomic coordinates corre-

**Table 1.** Unit cell volume and parameters at different temperatures for the investigated compounds in the  $R32$  phase

Crystal	$T$ , K	$a$ , Å	$\alpha$ , deg	$V$ , Å <sup>3</sup>
$\text{PrFe}_3(\text{BO}_3)_4$	0	6.152	103.78	208.59
	200	6.154	103.77	208.81
	300	6.157	103.75	209.22
	500	6.163	103.71	210.02
	1000	6.185	103.57	212.81
$\text{HoFe}_3(\text{BO}_3)_4$	0	6.097	103.90	202.59
	200	6.097	103.88	202.81
	300	6.101	103.87	203.13
	500	6.108	103.83	203.97
	1000	6.131	103.71	206.70
$\text{TbFe}_3(\text{BO}_3)_4$	0	6.107	103.89	203.68
	200	6.109	103.87	203.89
	300	6.111	103.86	204.22
	500	6.118	103.82	205.07
	1000	6.141	103.69	207.80
$\text{NdFe}_3(\text{BO}_3)_4$	0	6.143	103.80	207.56
	200	6.144	103.79	207.78
	300	6.147	103.78	208.11
	500	6.154	103.74	208.98
	1000	6.176	103.60	211.76
$\text{DyFe}_3(\text{BO}_3)_4$	0	6.101	103.89	203.09
	200	6.103	103.88	203.31
	300	6.106	103.87	203.63
	500	6.113	103.82	204.48
	1000	6.135	103.71	207.20

sponding to temperatures of 0, 200, 300, 500, and 1000 K (Table 1).

The significant changes in the total phonon spectra of the compounds under study with increasing temperature were observed only in the vicinity of the point  $\Lambda$ . The obtained partial phonon spectra with frequencies below 25 meV for the directions  $\Gamma \rightarrow \Lambda \rightarrow F$  and  $\Gamma \rightarrow Q \rightarrow \Lambda \rightarrow Z$  (the Brillouin zone and these directions are shown in Fig. 2) are presented in Fig. 3 for the  $\text{PrFe}_3(\text{BO}_3)_4$  and  $\text{NdFe}_3(\text{BO}_3)_4$  crystals and in Fig. 4 for the  $\text{TbFe}_3(\text{BO}_3)_4$ ,  $\text{DyFe}_3(\text{BO}_3)_4$ , and  $\text{HoFe}_3(\text{BO}_3)_4$  crystals.

The phonon spectra of the  $\text{PrFe}_3(\text{BO}_3)_4$  and  $\text{NdFe}_3(\text{BO}_3)_4$  crystals calculated at different temperatures appeared very similar. It can be seen in Fig. 3 that, with increasing temperature, no significant changes in the vicinity of the point  $\Lambda$  occur, but the deflection of the acoustic branch remains and is especially pronounced in the  $\Gamma \rightarrow Q \rightarrow \Lambda \rightarrow Z$  direction (Figs. 3b, 3d). It is well-known that the structural

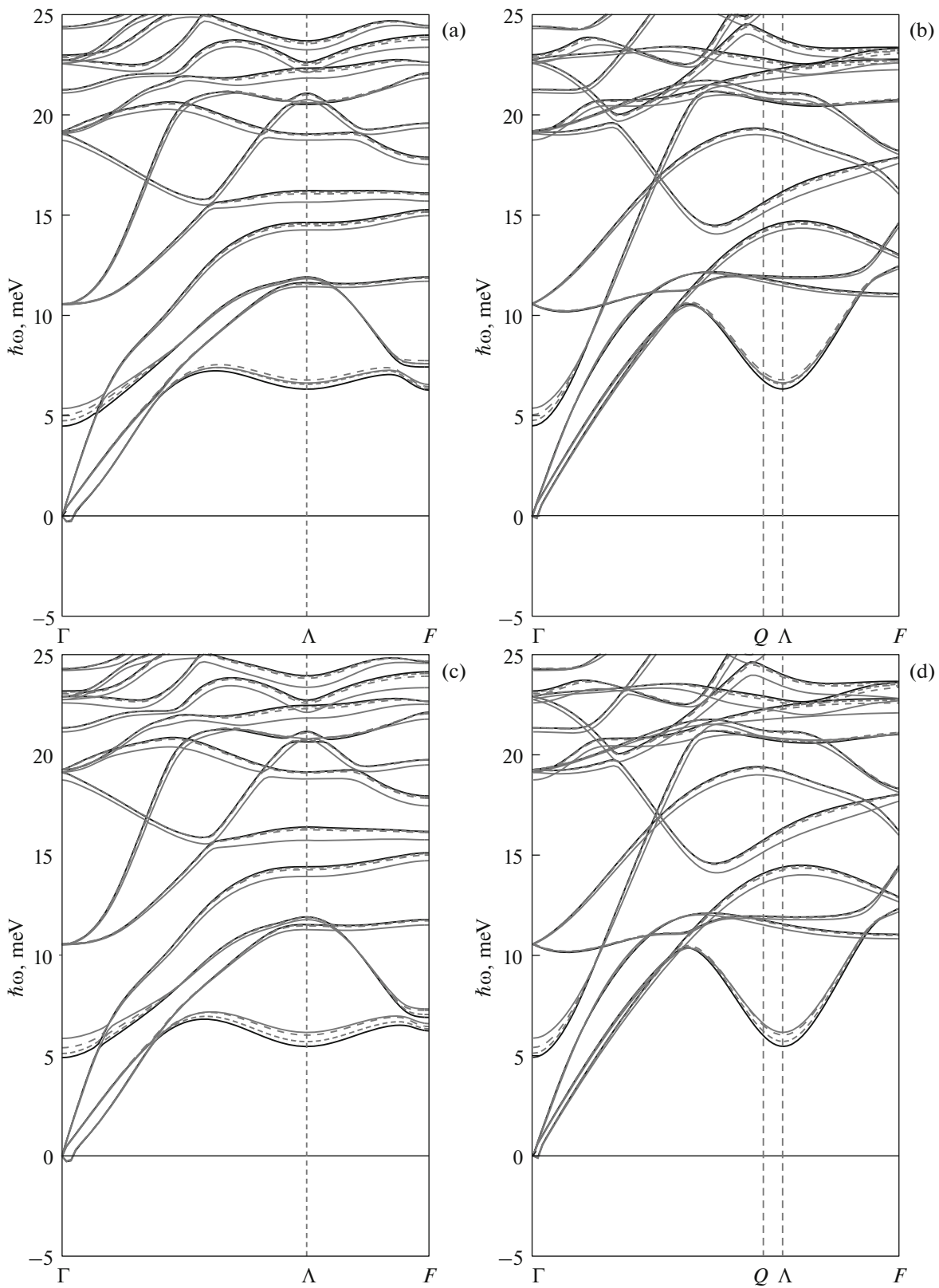


**Fig. 3.** Phonon spectra for (a, b) the  $\text{PrFe}_3(\text{BO}_3)_4$  and (c, d)  $\text{NdFe}_3(\text{BO}_3)_4$  crystals at temperatures of 0 (black solid line), 200 (gray dotted line), 300 (gray dashed line), 500 (gray dash-and-dot line), and 1000 K (gray solid line).

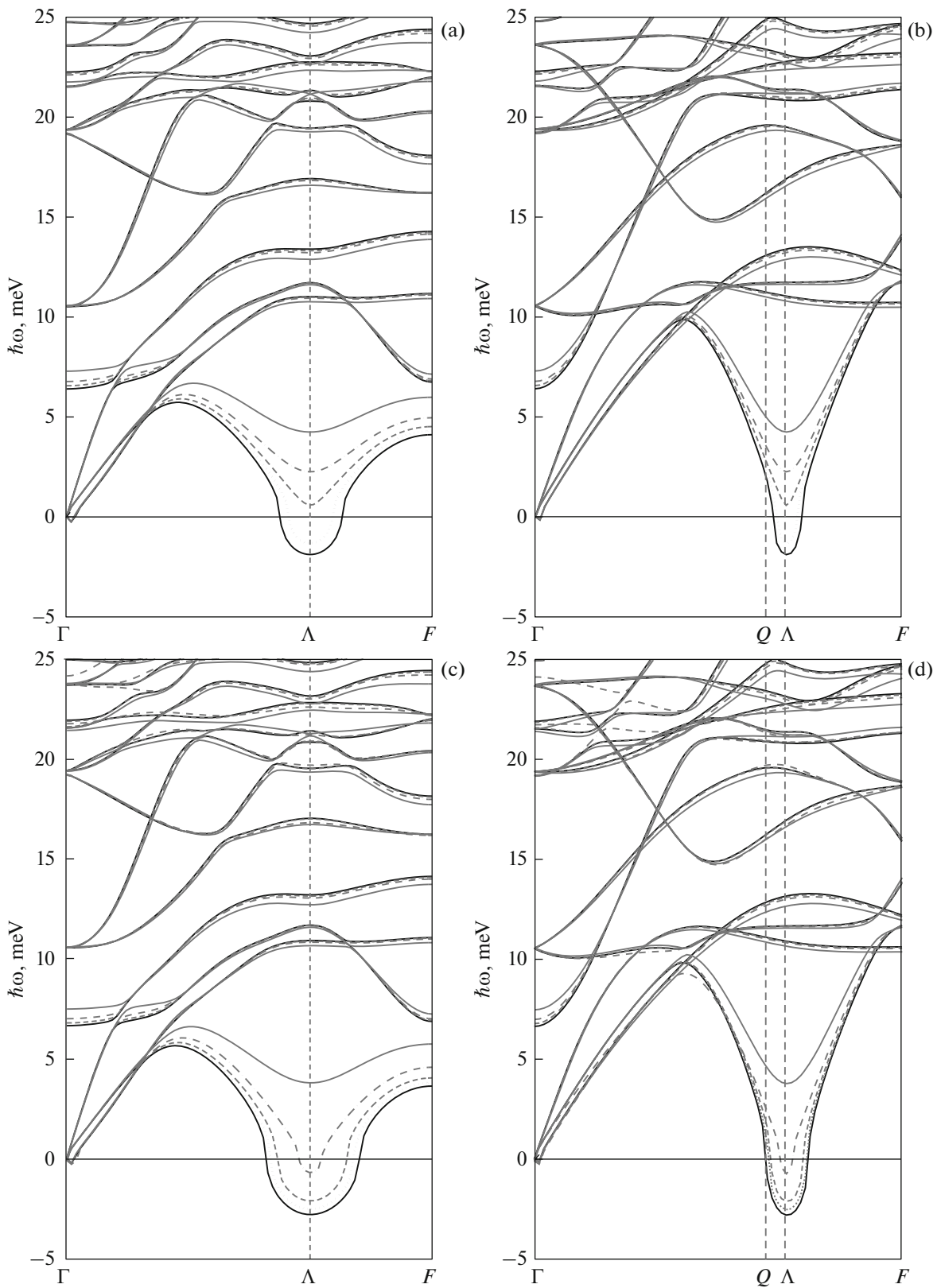


**Fig. 4.** Phonon spectra for (a, b) the  $\text{TbFe}_3(\text{BO}_3)_4$ , (c, d)  $\text{DyFe}_3(\text{BO}_3)_4$ , and (e, f)  $\text{HoFe}_3(\text{BO}_3)_4$  crystals at temperatures of 0 (black solid line), 200 (gray dotted line), 300 (gray dashed line), 500 (gray dash-and-dot line), and 1000 K (gray solid line). Imaginary modes are shown by negative values.

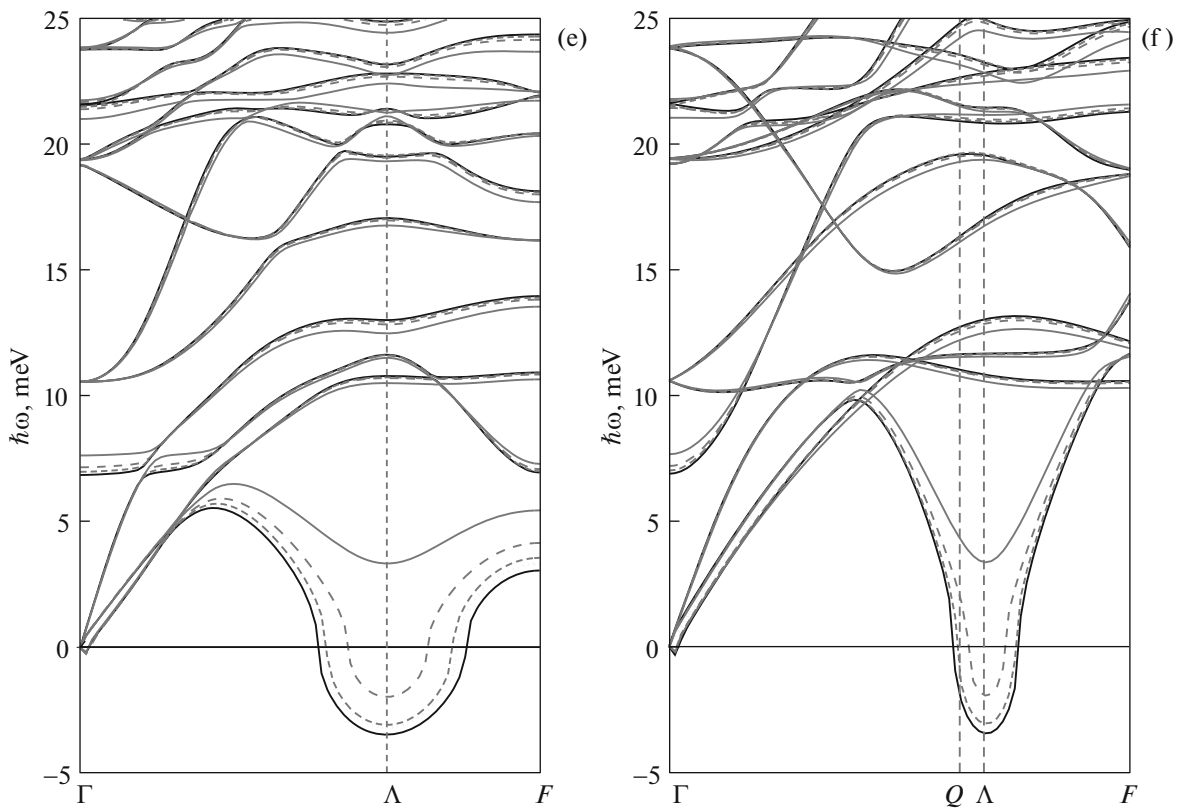
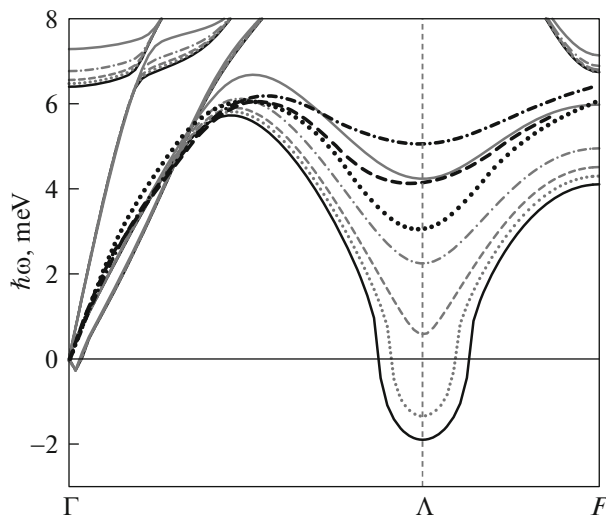


Fig. 4. (Contd.)



**Fig. 5.** Calculated dispersion dependences of the acoustic mode at temperatures of 0 (black solid line), 200 (gray dotted line), 300 (gray dashed line), 500 (gray dash-and-dot line), and 1000 K (gray solid line) and dependences obtained experimentally in [12] at temperatures of 198 (black dotted line), 250 (black dashed line), and 350 K (black dash-and-dot line). Imaginary modes are shown by negative values.

phase transition  $R32 \rightarrow P3_121$  is not observed in these compounds.

A quite opposite picture is observed in the  $\text{TbFe}_3(\text{BO}_3)_4$ ,  $\text{DyFe}_3(\text{BO}_3)_4$ , and  $\text{HoFe}_3(\text{BO}_3)_4$  crystals. As the temperature increases, the imaginary mode at the point  $\Lambda$  stabilizes and takes a real value in each crystal. In this case, in all the three crystals at a temperature of 1000 K, the frequency of the unstable mode takes similar values (3–4 meV) and, at 0 K, the absolute value of the unstable mode changes more strongly from one compound to another.

Figure 5 shows the dispersion dependences of the unstable acoustic mode for the  $\text{TbFe}_3(\text{BO}_3)_4$  crystal in the  $\Gamma \rightarrow \Lambda$  direction calculated in this study at temperatures from 0 to 1000 K and obtained experimentally from the inelastic neutron scattering spectra at temperatures of 198, 250, and 350 K in [7]. One can see that the calculated data are qualitatively consistent with the experiment.

The structural phase transition  $R32 \rightarrow P3_121$  in the  $\text{TbFe}_3(\text{BO}_3)_4$ ,  $\text{DyFe}_3(\text{BO}_3)_4$ , and  $\text{HoFe}_3(\text{BO}_3)_4$  crystals occurs at temperatures of 192, 282, and 369 K, respectively. In this study, we obtained using the quasi-harmonic approximation that the soft mode takes real values in  $\text{TbFe}_3(\text{BO}_3)_4$  at a temperature of about 300 K, in  $\text{DyFe}_3(\text{BO}_3)_4$  between 500 and

1000 K, and in  $\text{HoFe}_3(\text{BO}_3)_4$  between 500 and 1000 K. Certainly, this approach does not allow us to make a quantitative comparison with the experimental temperatures of the phase transitions in the crystals under study. The behavior of the low mode at the point  $\Lambda$  with increasing temperature in ferrobates with different types of a rare-earth ion are qualitatively consistent with the experimental dependence of the structural phase transition temperature on the type of a rare-earth ion.

Based on the results obtained for the  $\text{PrFe}_3(\text{BO}_3)_4$  and  $\text{NdFe}_3(\text{BO}_3)_4$  crystals, we may conclude that the deflection of the acoustic branch at the point  $\Lambda$  does not speak about the structural instability, at least in the framework of the approach used. Summarizing the obtained data on the behavior of the low-lying mode at the point  $\Lambda$  with increasing temperature, we can state that, at high temperatures, the deflection of the acoustic branch at the point  $\Lambda$  remains in all ferrobates with a huntite structure.

#### FUNDING

This study was supported by the Russian Science Foundation, project no. 17-72-10122.

#### CONFLICT OF INTEREST

The authors declare that they have no conflicts of interest.

#### REFERENCES

1. J. A. Campá, C. Cascales, E. Gutiérrez-Puebla, M. A. Monge, I. Rasines, and C. Ruíz-Valero, *Chem. Mater.* **9**, 237 (1997).
2. Y. Hinatsu, Y. Doi, K. Ito, M. Wakeshima, and A. Alemi, *J. Solid State Chem.* **172**, 438 (2003).
3. S. A. Klimin, D. Fausti, A. Meetsma, L. N. Bezmaternykh, P. H. M. van Loosdrecht, and T. T. M. Palstra, *Acta Crystallogr., Sect. B* **61**, 481 (2005).
4. D. Fausti, A. A. Nugroho, P. H. M. van Loosdrecht, S. A. Klimin, M. N. Popova, and L. N. Bezmaternykh, *Phys. Rev. B* **74**, 024403 (2006).
5. V. S. Kurnosov, V. V. Tsapenko, L. N. Bezmaternykh, and I. A. Gudim, *Low Temp. Phys.* **40**, 1087 (2014).
6. V. I. Zinenko, M. S. Pavlovskii, A. S. Krylov, I. A. Gudim, and E. V. Eremin, *J. Exp. Theor. Phys.* **117**, 1032 (2013).
7. M. S. Pavlovskiy, K. A. Shaykhutdinov, L. S. Wu, G. Ehlers, V. L. Temerov, I. A. Gudim, A. S. Shinkorenko, and A. Podlesnyak, *Phys. Rev. B* **97**, 054313 (2018).
8. M. S. Pavlovskii, V. I. Zinenko, and A. S. Shinkorenko, *JETP Lett.* **108**, 116 (2018).
9. A. Togo, L. Chaput, I. Tanaka, and G. Hug, *Phys. Rev. B* **81**, 174301 (2010).
10. G. Kresse and J. Furthmuller, *Phys. Rev. B* **54**, 11169 (1996).
11. J. P. Perdew, K. Burke, and M. Ernzerhof, *Phys. Rev. Lett.* **77**, 3865 (1996).
12. H. J. Monkhorst and J. D. Pack, *Phys. Rev. B* **13**, 5188 (1976).
13. S. L. Dudarev, G. A. Botton, S. Y. Savrasov, C. J. Humphreys, and A. P. Sutton, *Phys. Rev. B* **57**, 1505 (1998).
14. A. Togo and T. Tanaka, *Scr. Mater.* **108**, 1 (2015).

*Translated by E. Bondareva*